Indian Journal of Science and Technology, *Vol 10(29), DOI: 10.17485/ijst/2017/v10i29/117372, August 2017*
ISSN (Print) : 0974-6846
ISSN (Online) : 0974-5645

Geometrical Interruption in the Nerve Anatomical Model of the Foot to Simulate Small Fiber Neuropathy

M. Z. Ul Haque[1,2]*, Peng Du[2] and Leo K. Cheng[2]

[1]Department of Biomedical Engineering, Barrett Hodgson University, Karachi, Pakistan; muhammad.zeeshan@bhu.edu.pk
[2]Auckland Bioengineering Institute, University of Auckland, Auckland, New Zealand;

Abstract

Diabetic Foot Ulceration (DFU) is a type of Small Fiber Neuropathy (SFN) which usually arises in the unmyelinated smaller Intra-Epidermal Nerve Fibers (IENF) of the foot. Skin biopsy is a diagnostic method to examine quantitatively IENF in the foot but examination is limited to the specific positions of the body. Computational models may provide an alternative approach to examine SFN. Formerly, an anatomical model of Normal IENF (NIENF), based on IENF Density (IENFD) at various locations in the human foot was presented. Therefore, in this study, a geometrically Interrupted IENF (IIENF) model is developed using reduced IENFD, to simulate SFN at miscellaneous locations of the human foot. This IIENF model was then compared with the NIENF model for the same location of the foot and observed reduced IENF network in this IIENF model as compared to NIENF model. Furthermore, approximately 98% of the realistic IENF terminals at the skin were generated using the modified Monte Carlo Algorithm (MCA) and the reduced empirical IENFD at the various locations of the foot. This IIENF model provides a starting platform for evaluating diabetic foot ulceration. The IIENF model may be used in future studies for functional consequences by stimulating the most distal sensory IENF of the skin of the foot.

Keywords: Diabetic Foot Ulceration, Computational Model, Intra-Epidermal Nerve Fiber, Monte Carlo Algorithm, Skin Biopsy, Small Fiber Neuropathy

1. Introduction

A major organ in the human body is the skin and its main function includes sensory perception, thermoregulation, and host defense. Epidermis and dermis are the two larger layers of the skin[1–3]. The human skin comprises not only of encapsulated neural receptor but also consists of non-encapsulated free nerve terminals, called Intra-Epidermal Nerve Fibers (IENF) and they are present at the peripheral side of the sensory nerves[4]. IENF lose their myelin sheath as they traverse the dermal-epidermal intersection of the skin and are usually unmyelinated axons[4,5]. The IENF Density (IENFD) is an important quantitative measure to calculate the number of positive nerve fibers transferring the dermal-epidermal intersections per mm length of the epidermal surface. The IENFD remains mostly constant throughout the life of healthy subjects[4]. The IENFD is also likely to be determined by anatomical location and a general reduction in IENFD is often in relation to its distance from the dorsal root ganglion[4].

The major complication of the diabetes mellitus is Diabetic Foot Ulceration (DFU) with a life span increased risk of approximately 15-25 % larger in contrast to healthy foot[6,7]. Neuropathic and neuro-ischemic are the types of DFU with an occurrence rate of 50% each from diabetes patients[8]. International working group on diabetic foot and clinical guideline of the American diabetes association provide a general guideline for the improvement and prevention of DFU and that includes patient education, routine foot inspection, daily foot examination, glucose

*Author for correspondence

monitoring, lipid administration, blood pressure monitoring and curative foot wear[9–11]. The healing duration of DFU depends on incorporate standard care and etiologic factors[12]. Previous study suggested the average healing time courses of DFU was eight weeks[13]. Therefore, elevated efforts are required for the examination of DFU by performing diagnostic studies so that the risk of DFU is minimized.

Skin biopsy is a useful tool for determining the IENFD in DFU which involve small fiber neuropathy (SFN)[14,15]. This method is used for the morphological assessment of a diabetic patient when the peripheral nerve is damaged[16]. There is a decrease in IENFD, examined in diabetic neuropathy at various anatomical positions of the human foot[17–20]. It is not possible to obtain the empirical histological IENFD data from the entire foot skin in normal and DFU due to complex epidermal-dermal structures as well as large anatomical area[21]. Therefore, quantitative IENFD data offer a useful stage for the generation of synthetic IENF network on whole foot's skin by examining the IENF structure. It is done by using the bifurcated tree generation algorithm as mostly IENF have a bifurcated tree structure[21,22].

Therefore, in this study we modified our previously developed anatomical Normal IENF (NIENF) model using the revised Monte Carlo Algorithm (MCA)[21,23]. The modification was done by incorporating anatomical interruptions in the IENF model and literature based reduced IENFD data for diabetic neuropathy at miscellaneous locations of the nerves of the foot. This anatomical Interrupted IENF (IIENF) model also demonstrated the structural change in the IENF network during diabetic foot ulcer at the diverse location in the DFU[24].

2. Methodology

In our previous study, a comprehensive normal nerve anatomical model of the foot was developed[21,23]. The anatomical normal nerve model includes various larger nerves as well as smaller synthetic normal IENF structures in the foot. The larger nerve model was constructed from the Visible Human Male (VHM) along with anatomical representations[23], while the smaller NIENF structures was developed using modified description of MCA and IENFD facts on the different location of the normal foot[21,23].

An anatomically based IIENF model at the different position of the foot is proposed using the modified version of MCA and reduced IENFD to simulate SFN. For this purpose, following phases were included in the construction of the anatomically IIENF model.

2.1 Common Locations for Diabetic Foot Ulceration

The following locations of the foot model were selected for the development of the synthetic IIENF model as they are the most common locations for DFU[25].

- The lateral location of the foot close to the lateral malleolus was selected. This location has been suggested by the European Federation of Neurological Science (EFNS) with a sensitivity and specificity of approximately 75% for the quantification of IENFD for diagnosing length dependent peripheral neuropathy [19,26–28].
- The dorsal region just above the extensor brevis muscle was selected as there was a reduced IENFD observed in this exact location for a diabetic neuropathy patient[18].
- The medial malleolus region of the foot was chosen as this location was showed a reduced IENFD in diabetic neuropathy using skin biopsy[20].
- The metatarsal head region of the foot was selected since a majority of diabetic foot ulcers initially develop at this location[25].
- The plantar region of the great toe and the plantar heel side were also chosen since these sites were most frequently afflicted with diabetic foot ulcers[25].

2.2 Data Point Generation

The exterior surface of a 3D anatomical foot model developed previously by Fernandez et al.[29] acted as an input for the construction of the synthetic IIENF model. The foot model was represented as a 2D host mesh on which regular data points were distributed, as described by Fernandez[30]. The nerve terminals were generated through projection from the points to the exterior surfaces of the human foot model. These data points were generated with evenly spaced, regular computational points in the form of a square matrix on the exterior element of the human foot model. Here, the data points on the exterior areas were characterized with IENFD. The data points were computed from the IENFD on different areas of the foot, as deduced from anatomical study.

2.3 Anatomical IIENF Model

The modified MCA was employed for the development of anatomical IIENF model in the diverse locations of the foot[31]. This algorithm depends on the center of mass theory over the surface in a defined area and is explained in detail previously[23]. This algorithm was adapted due to its relative ease in generating the bifurcated tree structure for the predefined datum points and also less computationally expensive for the designated area of influence in 3D. Once the nerve terminals over the external surfaces of the different region in the foot model were generated, a bifurcated synthetic nerve tree was developed from each of the cutaneous branches in the various DFU locations. Later on, this initial bifurcated tree network was applied to develop the IENF interrupted network at different locations using modified MCA.

The synthetic anatomical IIENF model was then developed by employing revised MCA[31] at the various cutaneous distributions of the human foot. It was achieved by following the various diabetic foot locations for the dorsal and plantar sides of the normal and SFN. The developed synthetic comprehensive IENF model was based on IENFD data for the normal and the SFN patients. The previously selected parameter values were used for the construction of the IIENF structural model and these parameter are branching angle limit of 60°, branch length limit of 0.01 mm, branching fraction of 0.4 and a diameter of 1.5 μm[21]. These parameter values were selected in order to generate the rational number of nerve terminals in contrast to the computed number of nerve terminals and also utilized the majority of the data points of the specific region in the normal and diabetic foot[21].

3. Results

The sample interrupted computational data point's projection on the external dorsal great toe face of the foot model, based on the IENFD using cubic Hermite basis function is given in Figure 1. These data points are generated in the form of a regular grid scheme with equal space. The computational data points are evenly space in the local ξ-coordinate system as represented in Figure 1.

The developed anatomical IIENF model based on the IENFD for SFN was then compared with the NIENF model at the same region and their simulated results are presented in Table 2. Table 1 represents that the number of terminal branch generations, computed nerve terminals, and the produced nerve terminals are considerably reduced in this anatomical IIENF model as compared to the NIENF model in the same area of the foot with the same number of cutaneous nerve branches from the larger nerves of the foot in the normal healthy subjects.

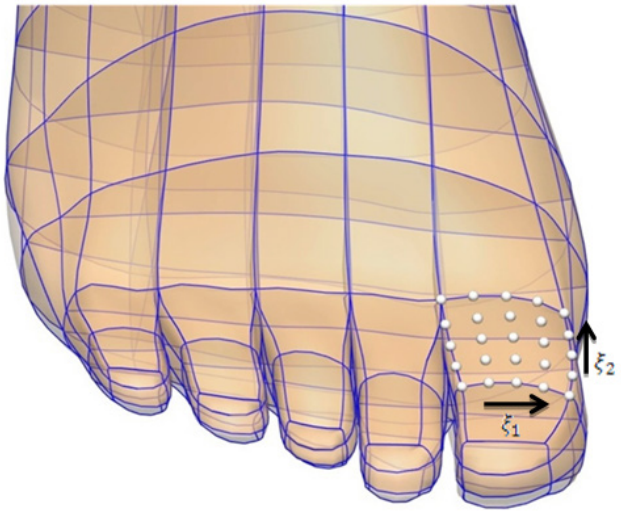

Figure 1. The computational data points with a 5 by 5 regular grid with equal space in the local ξ- coordinates using cubic Hermite basis function at one of the dorsal big toe regions of the foot.

The comprehensive synthetic anatomical IENF bifurcated model using the revised MCA is shown in Figure 2. This comprehensive anatomical model consists of the synthetic normal and interrupted IENF structures at various areas of the foot respectively. In addition, all the bones, muscles, larger nerves, as well as cutaneous segmentations of the several larger nerves in the human foot are also involved in this model. This comprehensive anatomical IENF model was also used to simulate structural changes in DFU at various locations of the foot.

4. Discussions

The IENFD quantitative data in the normal and SFN patients are limited for the various locations of the foot apart from plantar regions and these locations were aforementioned in section 2.1. In this study, the IENFD data for the plantar region was assumed as it was based on the fact that palmer or (non-hairy) surface of the hand is similar to the sole side of the foot[34]. Consequently, the proportion of 0.548 and 0.511 was selected to compute the IENFD at the plantar side of the normal and the dia-

Table 1. Comparison of the IENF network between the generated normal and interrupted synthetic IENF model at the various region depend on the IENFD of normal subjects and SFN patients

Parameters Region of the foot		IENFD (nerve terminals/ mm)	References	Number of cutaneous branches	Mean terminal branch generation	Computed number of nerve terminals	Generated number of nerve terminals
NIENF Model Simulation	Lateral Malleolus	17.30	(32)	2	18	22850	19983
	Lateral Little toe	17.30		1	16	4050	4045
	Medial Malleolus	11.91	(20)	2	17.5	10268	10319
	Medial Great Toe	11.91		2	15	2248	1891
	Plantar Region	11.6	Assumptions (26, 27)	23	11.65	7024	6819
	Great Toe	11.6		10	10.7	1189	1149
	Plantar Heel	11.6		9	10.7	1813	1529
	Dorsal Region	21.32	(18)	1	17	3669	3153
	Great Toe	21.32		5	13	3436	2794
	2nd Toe	21.32		4	12	2091	1858
	3rd Toe	21.32		4	12	1889	1821
	4th Toe	21.32		4	13	1805	1782
	5th Toe	21.32		4	11	1144	934
IIENF Model Simulation	Lateral Malleolus	3.3	(33)	2	13	784	711
	Lateral Little Toe	3.3		1	11	140	143
	Medial Malleolus	1.31	(20)	2	10	149	157
	Medial Great Toe	1.31		2	7	22	25
	Plantar Region	2.3	Assumptions (26, 27)	23	5.1	108	99
	Great Toe	2.3		10	5	37	32
	Plantar Heel	2.3		9	5	35	32
	Dorsal Region	2.18	(18)	1	10	75	80
	Great Toe	2.18		5	5.2	34	37
	2nd Toe	2.18		4	6	29	31
	3rd Toe	2.18		4	6	29	30
	4th Toe	2.18		4	6	28	28
	5th Toe	2.18		4	5.2	25	27

betic foot as these ratios was empirical between the hairy and non-hairy skin at the human wrist surface for the normal and SFN subjects[26,27]. Similarly, the number of nerve terminals in the different position of the normal as well as SFN patient was scaled by a portion of 100 so that a whole IENF model with a realistic nerve terminals were constructed computationally and the number of computed nerve terminals in the NIENF and IIENF models are mentioned in Table 1.

Although the modified MCA was able to construct a realistic number of nerve endings in different segments of the foot, there were still some smaller limitations in using this algorithm. The main limitation was that, it did not occupy the exact locations of the generated data points. Although it generated the nerve terminals in locations nearby the data points due to the branch length limit was larger than the selected length limit and therefore, terminated at the closest data points locations. Also, the number of calculated nerve terminals was scaled by a factor of 100 in order to reduce the computational time for the generated IENF structures, although the generated nerve terminals were approximately 98% of the scaled nerve terminals. The

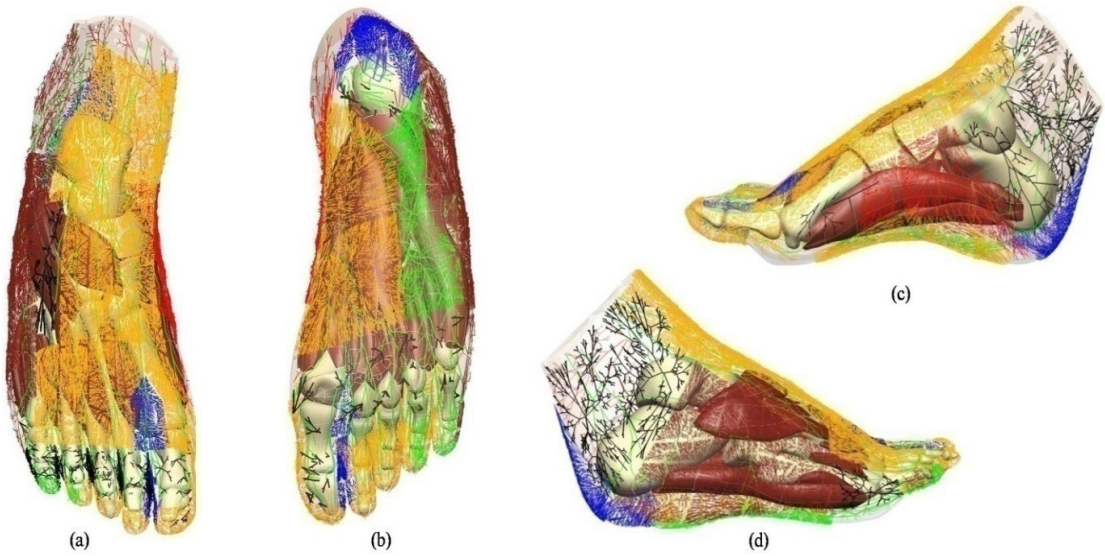

Figure 2. Different aspects of the synthetic NIENF and IIENF structures at various regions of the larger nerve model including muscles and bones: (a) Dorsal view of the cutaneous allocation of the various dorsal nerves including the IIENF model above the flexor retinaculum muscles as well as at the various dorsal toes. The interrupted dorsal nerves cutaneous distribution are represented by the black color while the normal Superficial Peroneal Nerve (SPN) and Sural Nerve (SN) cutaneous distributions are illustrated by the golden and maroon colors respectively. (b) Plantar view of the cutaneous segmentation of the Medial Plantar Nerve (MPN), Lateral Plantar Nerve (LPN) and Medial Calcaneal Nerves (MCN) defined by golden, green and blue colors respectively, while the IIENF structure at the MCN, each metatarsal area, and at the great toe, illustrated by the black colors. (c) Medial view of synthetic IENF model representing cutaneous distribution in normal (red) and interrupted (black) saphenous nerve (SaN) model. (d) Lateral view of the cutaneous segmentation of the normal (maroon) and the interrupted (black) synthetic IENF model.

number of generated nerve terminals at some locations did not match the scaled nerve terminals.

Future research should focus on refining this algorithm so that it may be used to examine the structural changes in the IENF network by producing an accurate number of generated nerve terminals in conjunction with the computed number of nerve terminals. The generated IENF network resolution could be enhanced by decreasing the scaling to 50 or less so that it may generate more nerve terminals at the foot's surface. This will help to create a more realistic biological IENF network that has a greater number of nerve terminals at the surface of the foot. Furthermore, future research should focus on developing the synthetic dermal plexus and various types of mechanoreceptors and these could be incorporated with the free nerve terminals so as to construct an additionally realistic anatomical nerve model in the foot's skin.

5. Conclusions

A complete anatomical IIENF model was developed to simulate the DFU in the various locations of the human foot. The empirical reduced IENFD at different region of the foot was used in this IIENF model. The reduced number of generated nerve terminals was observed in this anatomical IIENF model as compared to the NIENF nerve model in the similar location of the foot with the same number of cutaneous nerve branches from the larger nerves of the foot. The simulation study confirmed that approximately 98% of the realistic IENF terminals at the skin of the foot were generated using the modified MCA and the empirical IENFD at the various locations of the foot. This IIENF model creates the groundwork for simulating DFU in prospective studies, where it may provide tools to clinicians and physiologists for examining structural consequences of diabetic neuropathy in its initial stages.

6. Acknowledgements

The authors would like to acknowledge Dr. Justin Fernandez and Prof. Merryn Tawhai for guiding in the construction of the anatomical nerve model. The authors also acknowledge the financial support provided by New Economy Research Fund of New Zealand.

7. References

1. Langer K. On the anatomy and physiology of the skin: II. Skin Tension (With 1 Figure). British Journal of Plastic Surgery. 1978; 31(2):93–106. Crossref
2. Xu F, Lu T, Seffen K. Biothermomechanics of skin tissues. Journal of the Mechanics and Physics of Solids. 2008; 56(5):1852–84. Crossref
3. Xu F, Wen T, Seffen K, Lu T. Modeling of skin thermal pain: A preliminary study. Applied Mathematics and Computation. 2008; 205(1):37–46. Crossref
4. Lauria G, Devigili G. Skin biopsy as a diagnostic tool in peripheral neuropathy. Nature Clinical Practice Neurology. 2007; 3(10):546–57. PMid: 17914343. Crossref
5. Bear MF, Connor BW, Paradiso MA. The somatic sensory system. Neuroscience: Exploring the Brain. 3rd ed. Lippincott Williams and Wilkins; 2007.
6. Boulton AJM, Kirsner RS, Vileikyte L. Neuropathic diabetic foot ulcers. New England Journal of Medicine. 2004; 351(1):48–55. PMid: 15229307. Crossref
7. Rathur HM, Boulton AJM. The neuropathic diabetic foot. Nature Clinical Practice Endocrinology and Metabolism. 2007; 3(1):14–25. PMid: 17179926. Crossref
8. Forlee M. What is the diabetic foot? The rising prevalence of diabetes worldwide will mean an increasing prevalence of complications such as those of the extremities. Continuing Medical Education. 2010; 28(4):152–6.
9. Association AD. Microvascular complications and foot care. Diabetes Care. 2016; 39(Supplement 1):S72–80. PMid: 26696685. Crossref
10. Bus S, Netten J, Lavery L, Monteiro-Soares M, Rasmussen A, Jubiz Y, et al. IWGDF guidance on the prevention of foot ulcers in at-risk patients with diabetes. Diabetes/Metabolism Research and Reviews. 2016; 32(S1):16–24. PMid: 26334001. Crossref
11. Iraj B, Khorvash F, Ebneshahidi A, Askari G. Prevention of diabetic foot ulcer (DFU). International Journal of Preventive Medicine. 2013; 4(3):373–6.
12. Zimny S, Schatz H, Pfohl M. Determinants and estimation of healing times in Diabetic Foot Ulcers. Journal of Diabetes and its Complications. 2002; 16(5):327–32. Crossref
13. Robertshaw L, Robertshaw DA, Whyte I. Audit of time taken to heal diabetic foot ulcers. Practical Diabetes International. 2001; 18(1):6–9. Crossref
14. Park TS, Baek HS, Park JH. Advanced diagnostic methods of small fiber diabetic peripheral neuropathy. Diabetes Research and Clinical Practice. 2007; 77(3):S190–3. PMid: 17481766. Crossref
15. Jude E, Blakytny R, Bulmer J, Boulton A, Ferguson M. Transforming growth factor-beta 1, 2, 3 and receptor type I and II in diabetic foot ulcers. Diabetic Medicine. 2002; 19(6):440–7. PMid: 12060054. Crossref
16. Loseth S, Lindal S, Stalberg E, Mellgren S. Intraepidermal nerve fibre density, quantitative sensory testing and nerve conduction studies in a patient material with symptoms and signs of sensory polyneuropathy. European Journal of Neurology. 2006; 13(2):105–11. PMid: 16490039. Crossref
17. Bakotic BW. Epidermal nerve fiber density testing: An overview. Podiatry Management; 2010. p. 141–52.
18. Wendelschafer-Crabb G, Kennedy W, Walk D. Morphological features of nerves in skin biopsies. Journal of the Neurological Sciences. 2006; 242(1):15–21. PMid: 16448669. Crossref
19. Lauria G, Cornblath D, Johansson O, McArthur J, Mellgren S, Nolano M, et al. EFNS guidelines on the use of skin biopsy in the diagnosis of peripheral neuropathy. European Journal of Neurology. 2005; 12(10):747–58. PMid: 16190912. Crossref
20. Hirai A, Yasuda H, Joko M, Maeda T, Kikkawa R. Evaluation of diabetic neuropathy through the quantitation of cutaneous nerves. Journal of the Neurological Sciences. 2000; 172(1):55–62. Crossref
21. Ul Haque MZ, Du P, Cheng LK, Jacobs M. An anatomically realistic geometrical model of the intra-epidermal nerves in the human foot. The 15th International Conference on Biomedical Engineering; Springer. 2014. Crossref
22. Olsbo V. Analysis and modeling of epidermal nerve fiber patterns: A point process approach. 2006.
23. Ul Haque MZ, Du P, Cheng LK, Jacobs MD. An anatomically-based model of the nerves in the human foot. World Academy of Science, Engineering and Technology. 2012; 69:451–5.
24. Krishnan ST, Baker NR, Carrington AL, Rayman G. Comparative roles of microvascular and nerve function in foot ulceration in type 2 diabetes. Diabetes Care. 2004; 27(6):1343–8. PMid: 15161786. Crossref
25. Thompson E. Locations of foot ulcers: Diabetes Health Center; 2011 [updated June 29, 2011]. Available from: http://diabetes.webmd.com/locations-of-foot-ulcers.
26. Thomsen N, Bjorkman A, Dahlin LB. Diabetic neuropathy–nerve morphology in the upper extremity. Recent Advances in the Pathogenesis, Prevention and Management of Type 2 Diabetes and its Complications, ed 2011; 2011 Aug 29. p. 33–42.
27. Thomsen N, Englund E, Thrainsdottir S, Rosen I, Dahlin L. Intraepidermal nerve fibre density at wrist level in diabetic and non-diabetic patients. Diabetic Medicine. 2009; 26(11):1120–6. PMid: 19929990. Crossref
28. Lacomis D. Small-fiber neuropathy. Muscle and Nerve. 2002; 26(2):173–88. PMid: 12210380. Crossref
29. Fernandez J, Ul Haque M, Hunter P, Mithraratne K. Mechanics of the foot Part 1: A continuum framework for evaluating soft tissue stiffening in the pathologic foot. International Journal for Numerical Methods in Biomedical

Engineering. 2012 Oct; 28(10):1056–70. PMid: 23027635. Crossref
30. Fernandez JW. An anatomically based finite element model of patella articulation: Towards a diagnostic tool. Biomedical Engineering, University of Auckland; 2004.
31. Tawhai MH, Pullan A, Hunter P. Generation of an anatomically based three-dimensional model of the conducting airways. Annals of Biomedical Engineering. 2000; 28(7):793–802. Crossref
32. Arthur RP, Shelley WB. The innervation of human epidermis. The Journal of Investigative Dermatology. 1959; 32(3):397. PMid: 13641817. Crossref
33. Ebadi H, Perkins BA, Katzberg HD, Lovblom LE, Bril V. Evaluation of proxy tests for SFSN: Evidence for mixed small and large fiber dysfunction. PloS one. 2012; 7(8):e42208. PMid: 22870304, PMCid: PMC3411719. Crossref
34. Anatomy/Terminology 2015. Available from: https://en.wikiversity.org/wiki/Anatomy/Terminology